

# Comparison between Thallium-201 and Technetium-99m-Tetrofosmin Uptake with Sustained Low Flow and Profound Systolic Dysfunction

Bruce A. Koplán, George A. Beller, Mirta Ruiz, Joo Y. Yang, Denny D. Watson and David K. Glover  
*Experimental Cardiology Laboratory, Cardiovascular Division, Department of Medicine, University of Virginia Health Sciences Center, Charlottesville, Virginia*

Technetium-99m-tetrofosmin uptake was compared to that of  $^{201}\text{Tl}$  in the setting of low flow and systolic dysfunction. **Methods:** In nine open-chested dogs, a severe left anterior descending (LAD) coronary artery stenosis resulted in a 54.3% mean flow reduction and decreased left ventricular thickening from  $21\% \pm 1\%$  to  $-3 \pm 2\%$ . After 30 min, 37 MBq (1 mCi) of  $^{201}\text{Tl}$  and microspheres were injected and initial and 2-hr redistribution images acquired. Two hours later, 370 MBq (10 mCi) of  $^{99\text{m}}\text{Tc}$ -tetrofosmin and microspheres were injected and an image was obtained. LAD:left circumflex (LCx) count ratios for both tracers and flows were calculated by well counting postmortem, and  $^{201}\text{Tl}$  and  $^{99\text{m}}\text{Tc}$ -tetrofosmin defect magnitudes were determined by quantitative image analysis. **Results:** LAD:LCx flow ratios were similar during  $^{201}\text{Tl}$  and  $^{99\text{m}}\text{Tc}$ -tetrofosmin injections ( $0.48 \pm 0.04$  versus  $0.49 \pm 0.05$ ,  $p = \text{n.s.}$ ). Final  $^{201}\text{Tl}$  activity ( $0.66 \pm 0.04$ ) was significantly higher than  $^{99\text{m}}\text{Tc}$ -tetrofosmin ( $0.55 \pm 0.05$ ;  $p < 0.05$ ). LAD/LCx  $^{99\text{m}}\text{Tc}$ -tetrofosmin image defect count ratio was similar to  $^{201}\text{Tl}$  defect count ratio on the initial rest  $^{201}\text{Tl}$  scan ( $0.57 \pm 0.03$  versus  $0.56 \pm 0.02$ ,  $p = \text{ns}$ ), but significantly less than  $^{201}\text{Tl}$  defect count ratio at 2 hr ( $0.57 \pm 0.03$  versus  $0.65 \pm 0.02$ ,  $p < 0.05$ ). **Conclusion:** In a low-flow model with profound systolic dysfunction, myocardial  $^{99\text{m}}\text{Tc}$ -tetrofosmin uptake was less than 2-hr redistribution  $^{201}\text{Tl}$  uptake; yet substantial  $^{99\text{m}}\text{Tc}$ -tetrofosmin uptake ( $>50\%$ ) reflective of viability was observed in the asynergic zone perfused by the stenotic LAD.

**Key Words:** thallium-201; technetium-99m-tetrofosmin; radionuclide imaging; myocardial ischemia

**J Nucl Med 1996; 37:1398-1402**

Technetium-99m-1,2-bis[bis(2-ethoxyethyl)phosphino]ethane ( $^{99\text{m}}\text{Tc}$ -tetrofosmin) is a new lipophilic cationic complex that, like  $^{201}\text{Tl}$  and  $^{99\text{m}}\text{Tc}$ -sestamibi, has been shown to clear rapidly from the blood after intravenous injection and be taken up by myocardial tissue in proportion to blood flow and tissue viability (1-3). Compared to  $^{201}\text{Tl}$ ,  $^{99\text{m}}\text{Tc}$ -complexed agents like  $^{99\text{m}}\text{Tc}$ -tetrofosmin have certain advantages, including a higher gamma energy photopeak and a shorter half-life, which allow for optimal radiation dosimetry and greater image contrast (4). Like  $^{99\text{m}}\text{Tc}$ -sestamibi, bolus administration of  $^{99\text{m}}\text{Tc}$ -tetrofosmin permits first-pass radionuclide ventriculography, and the combined assessment of perfusion and function may enhance its diagnostic ability (5). A recent multicenter trial reported comparable sensitivity and specificity between  $^{201}\text{Tl}$  and  $^{99\text{m}}\text{Tc}$ -tetrofosmin for detection of coronary artery disease (CAD) employing exercise planar imaging (6).

Like  $^{99\text{m}}\text{Tc}$ -sestamibi,  $^{99\text{m}}\text{Tc}$ -tetrofosmin clears slowly from the myocardium and, in experimental and clinical studies, it has shown little or no redistribution (3,7-9). Because of this negligible redistribution,  $^{99\text{m}}\text{Tc}$ -tetrofosmin imaging may have

limitations for the assessment of myocardial viability in hibernating myocardium. Experimental and clinical studies investigating the utility of  $^{99\text{m}}\text{Tc}$ -sestamibi imaging for detection of viability in zones of myocardial asynergy have yielded conflicting results. Some studies have suggested a lower detection rate of viable myocardium for  $^{99\text{m}}\text{Tc}$ -sestamibi compared to  $^{201}\text{Tl}$  or PET, whereas other studies have shown comparable  $^{201}\text{Tl}$  and  $^{99\text{m}}\text{Tc}$ -sestamibi uptake on quantitative SPECT imaging in patients with severe CAD and left ventricular (LV) dysfunction. In the Phase III multicenter  $^{99\text{m}}\text{Tc}$ -tetrofosmin trial, there was a 13% greater detection of ischemia or ischemia with scar with  $^{201}\text{Tl}$  than with  $^{99\text{m}}\text{Tc}$ -tetrofosmin (6). Tamaki et al. (10), however, showed that reversible perfusion abnormalities were similar between stress-rest  $^{99\text{m}}\text{Tc}$ -tetrofosmin and stress-delayed  $^{201}\text{Tl}$  images using SPECT imaging. Accordingly, the purpose of the present study was to compare rest and delayed  $^{201}\text{Tl}$  uptake with  $^{99\text{m}}\text{Tc}$ -tetrofosmin uptake for assessment of myocardial viability in a canine model of reduced coronary flow and severe LV systolic dysfunction.

## MATERIALS AND METHODS

### Surgical Preparation

The surgical preparation employed for these experiments has been previously described (11). Nine dogs (mean weight  $20.2 \pm 1$  kg) were anesthetized with sodium pentobarbital (30 mg/kg), intubated and ventilated on a respirator (Harvard Apparatus, South Natick, MA). The left femoral vein was cannulated with an 8F polyethylene catheter for administration of fluids, medications and radionuclides. Both femoral arteries were isolated and cannulated with 8F polyethylene catheters for blood pressure monitoring, collection of arterial blood samples and microsphere reference blood withdrawal. A Millar pressure catheter was advanced via the carotid artery to the LV cavity for determination of LV dP/dt. The ventilator was adjusted and bicarbonate administered to maintain blood gases within the normal physiologic range.

A thoracotomy was performed at the fifth intercostal space, and the heart was suspended in a pericardial cradle. A flare-tipped polyethylene catheter was inserted into the left atrial appendage for pressure measurement and injection of microspheres. A 1.5-cm proximal segment of both the left anterior descending (LAD) and the left circumflex artery (LCx) was dissected free of the epicardium. Ultrasonic flow probes (T201, Transonic Systems Inc., Ithaca, NY) were placed on the LAD and LCx coronary arteries. A snare ligature was then placed proximal to the probe. Two Doppler sonomicrometer crystals were sutured to the epicardial surface of the heart in regions supplied by the LAD and LCx arteries, respectively, to measure regional wall thickening. An eight-channel strip-chart recorder was used to monitor lead II of the electrocardiogram, arterial and left atrial pressures, ultrasonic LAD and LCx flows, regional LAD and LCx systolic wall thickening, LV pressure and LV dP/dt. All experiments were performed with

Received June 5, 1995; revision accepted Sept. 21, 1995.

For correspondence or reprints contact: David K. Glover, Experimental Cardiology Laboratory, Cardiovascular Division, Department of Medicine, Box 500, University of Virginia Health Sciences Center, Charlottesville, VA 22908.

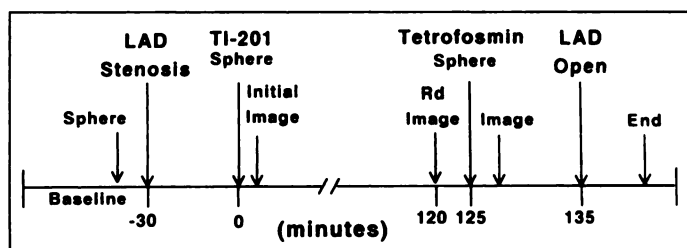


**FIGURE 1.** Experimental protocol. LAD = left anterior descending coronary artery; sphere = radioactive microsphere; Rd = 2-hr redistribution.

the approval of the University of Virginia Animal Research Committee, in compliance with the position of the American Heart Association on use of research animals.

### Preparation of Technetium-99m-Tetrofosmin

Technetium-99m-tetrofosmin was prepared from a freeze-dried kit provided in a 10-ml glass vial stored at 2° to 8°C. The vial was reconstituted with 5 ml of a sodium pertechnetate solution by diluting the eluate from a <sup>99m</sup>Tc generator with 0.9% saline. The vial was then shaken gently to ensure complete dissolution of the lyophilized powder and allowed to stand at room temperature for 15 min. Using ascending chromatography, mean radiochemical purity for the nine experiments was 96% ± 2%.

### Experimental Protocol

Figure 1 depicts the experimental protocol. After a 20-min baseline period, the snare ligature was adjusted to reduce LAD flow by 50% as measured by the flow probe. Thirty minutes later, 37 MBq (1 mCi) of <sup>201</sup>Tl was injected. Initial and redistribution <sup>201</sup>Tl images were acquired at 5 min and 2 hr postinjection. After the redistribution <sup>201</sup>Tl image was acquired, 370 MBq (10 mCi) of <sup>99m</sup>Tc-tetrofosmin was injected and an image was obtained in the technetium window 5 min later. After completion of this image (5-min acquisition time), the stenosis was released to demonstrate recovery of function. The time between <sup>99m</sup>Tc-tetrofosmin injection and release of the stenosis was 10 min. Because myocardial tissue activity is near maximal by 5 min postinjection, this protocol allowed ample time for uptake of this agent.

To determine the area at risk, the LAD was then occluded and monastral blue dye was injected into the left atrium. The dogs were then immediately euthanized with a lethal dose of potassium chloride and sodium pentobarbital. Radiolabeled microspheres were injected at baseline, with <sup>201</sup>Tl administration and with <sup>99m</sup>Tc-tetrofosmin injection for measurement of regional myocardial flow at these time points. The microspheres used in these experiments were either <sup>113</sup>Sn, <sup>103</sup>Ru, <sup>95</sup>Nb or <sup>46</sup>Sc.

### Postmortem Analysis

At the end of the experiment, the heart was excised and sliced evenly from apex to base into four segments as previously described (12). The left ventricle and septum were then separated from the remainder of the heart and photographed. Each slice was then carefully traced on acetate sheets to define the endocardial and epicardial borders, and the area at risk. Slices were subsequently incubated in 1% phosphate-buffered triphenyl tetrazolium chloride (TTC) solution for 10 min to define infarct size, then rephotographed and retraced on the same acetate sheets. Using a digital planimeter program, risk area and infarct area were determined.

### Determination of Regional Myocardial Blood Flow Using Radioactive Microspheres and Quantification of Tracer Uptake

The technique used in our laboratory for quantification of regional myocardial blood flow using radioactive microspheres has been previously described (13). A dose of spheres (2–5 million; mean diameter 11 μm) was suspended in 10% dextran and Tween

80. Normal saline was added to bring the total volume to 3 ml. Uniform mixing was accomplished initially by mechanical agitation followed by hand agitation between two syringes attached by a three-way stopcock. The microspheres were administered over 15 sec into the left atrium. For flow determination, paired arterial reference samples were obtained by continuous withdrawal over 130 sec, beginning 10 sec before the injection of each set of spheres. Each of the four myocardial slices was divided into eight transmural sections which were further subdivided into epicardial, midwall and endocardial segments, resulting in a total of 96 myocardial segments for each dog. The myocardial segments and arterial blood samples were counted for <sup>99m</sup>Tc-tetrofosmin activities in a gamma-well scintillation counter within 24 hr using a window setting of 120–160 keV. Forty-eight hours later, when the <sup>99m</sup>Tc activity had decayed, the myocardial and blood samples were counted for <sup>201</sup>Tl activity using a window setting of 50–100 keV. Three weeks later, when <sup>201</sup>Tl activity was negligible, the myocardial samples were counted a third time for microsphere regional blood flow determination. The microsphere window settings were: <sup>113</sup>Sn, 340–440 keV; <sup>103</sup>Ru, 450–550 keV; <sup>95</sup>Nb, 640–840 keV; and <sup>46</sup>Sc, 842–1300 keV. Tissue counts were corrected for background, decay and isotope spillover and regional myocardial blood flow calculated using computer software developed for this purpose (PCGERDA, Packard Instruments, Downers Grove, IL). The transmural regional flow values for a specific sample were derived from the weighted average of epicardial, midwall and endocardial values for that sample. To facilitate comparisons between tracer activity and flow, the <sup>201</sup>Tl and <sup>99m</sup>Tc-tetrofosmin activities and microsphere flows were normalized to the average value of 15–18 samples taken from the nonischemic region supplied by the LCx.

### Image Acquisition and Quantification of Defect Count ratio

All images were recorded for 5 min in the left lateral projection with a standard nuclear medicine gamma camera and computer (Technicare 420, Ohio Nuclear, Solon, OH). An all-purpose, low-to-medium energy collimator with a 20% window centered around the photopeak of <sup>99m</sup>Tc, and a 25% window centered around the photopeak of <sup>201</sup>Tl were used. Prior to imaging, a lead shield was placed over the abdomen to reduce liver and splanchnic activity.

Prior to defect quantification, tissue cross-talk was minimized, using the modified background correction algorithm developed by the University of Virginia Clinical Nuclear Cardiology Lab (14,15).

For quantification of <sup>99m</sup>Tc activity, regions of interest (ROIs) were drawn on the defect area of the anteroseptal LV wall, and on the normally-perfused posterior wall of each image. ROIs were drawn to encompass as great an amount of the region in question without including border areas. The serial <sup>201</sup>Tl and <sup>99m</sup>Tc images were aligned, and average counts were taken from the same regions on each image. The in vivo defect ratio was computed by dividing the average counts per pixel in the ischemic region by the average counts per pixel in the nonischemic region.

### Statistical Analysis

Computations were performed using Systat software (Systat Inc., Evanston, IL). Results are expressed as mean values ± 1 s.e.m.. Differences were determined using univariate repeated measures analysis of variance, followed by appropriate post hoc comparisons. Differences were considered significant at a p value of <0.05 (two tailed).

## RESULTS

### Hemodynamics

Table 1 summarizes the mean heart rate, systemic arterial pressure and left atrial pressure, measured at baseline, during

**TABLE 1**  
Hemodynamic Parameters

	Baseline	Stenosis	
		<sup>201</sup> Tl	<sup>99m</sup> Tc-tetrofosmin
Heart rate (bpm)	122 ± 4	118 ± 6	106 ± 6*
Arterial pressure (mm Hg)	101 ± 3	104 ± 3	96 ± 3
Left atrial pressure (mm Hg)	9 ± 1	10 ± 1	12 ± 1

Values are mean ± s.e.m.  
\*p < 0.01 versus time of <sup>201</sup>Tl injection.

injection of each radionuclide and after release of the LAD stenosis. Note that between the time points when <sup>201</sup>Tl and <sup>99m</sup>Tc-tetrofosmin were injected, no significant differences in mean arterial pressure or left atrial pressure were observed, although there was a slight but significant decrease in heart rate from 118 ± 6 to 106 ± 6 bpm (p < 0.01). Therefore, hemodynamic conditions were comparable at the times when <sup>201</sup>Tl and <sup>99m</sup>Tc-tetrofosmin were injected.

#### Ultrasonic Flows

Changes in mean coronary ultrasonic flows are shown in Figure 2. Setting the stenosis resulted in a decrease in mean LAD flow from 23 ± 1 to 10 ± 1 ml/min (p < 0.001), and this flow level remained constant during the injection of both <sup>201</sup>Tl (10 ± 1) and <sup>99m</sup>Tc-tetrofosmin (10 ± 1, p = n.s.). After release of the stenosis, LAD flow stabilized at 33 ± 5 ml/min. No significant differences in LCx flow were observed during the experiment.

#### Wall Thickening

Figure 3 shows that the LAD stenosis resulted in a decrease in mean systolic wall thickening in the LAD territory from 21 ± 1% to -3 ± 2% (p < 0.001). No significant difference in LAD wall thickening occurred between injection of <sup>201</sup>Tl and <sup>99m</sup>Tc-tetrofosmin (-3 ± 2% versus -1 ± 2%, p = ns). After the stenosis was released, mean LAD wall thickening rose to 10 ± 4% (p = 0.001 versus wall thickening at <sup>99m</sup>Tc-tetrofosmin injection), indicating partial recovery of function with restoration of flow. No significant differences were noted in regional LCx thickening at baseline (18 ± 2%), during <sup>201</sup>Tl (19 ± 1%) or <sup>99m</sup>Tc-tetrofosmin injection (20 ± 1%), or with release of the stenosis (23 ± 3%). Therefore, the myocardium in the ischemic region became dyskinetic after the stenosis was set, remained stable at this level of dyskinesia throughout the times of injections of both tracers and showed nearly immediate recovery after release of the stenosis.

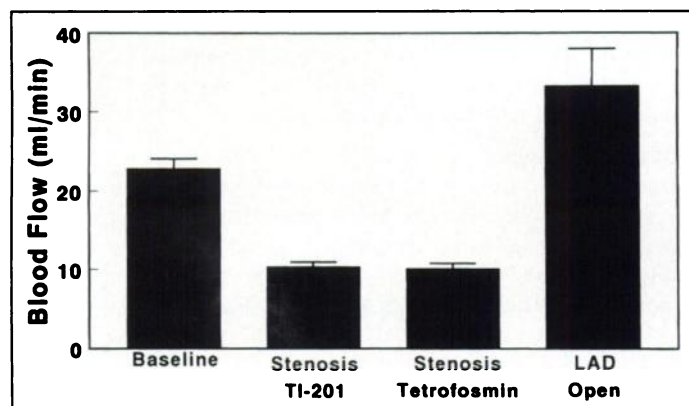


**FIGURE 2.** Ultrasonically-measured flow in the LAD coronary artery at serial time points. Note that flow remained constant at the time points when <sup>201</sup>Tl and <sup>99m</sup>Tc-tetrofosmin were injected.

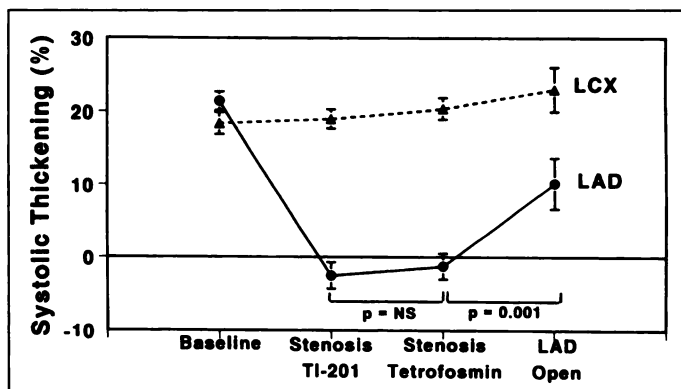


**FIGURE 3.** Serial changes in left ventricular systolic thickening at baseline, during <sup>201</sup>Tl and <sup>99m</sup>Tc-tetrofosmin injections with the LAD coronary artery stenosis in place, and after releasing the LAD stenosis. Note that percent thickening in the LAD zone increased significantly after releasing the stenosis, indicating the presence of viable myocardium. LCX = left circumflex coronary artery.

#### Risk Area and Infarct Size

Figure 4 displays mean risk area and infarct size expressed as a percent of the left ventricle. Mean infarct size was 2 ± 2%, and mean risk area was 29 ± 2% of the left ventricle. In six of the nine dogs, infarct size was less than 1% of the left ventricle. These data, along with the recovery of function shown in Figure 3, demonstrates that this canine model is one of predominantly viable but hypoperfused myocardium.

#### Myocardial Blood Flow

As shown in Figure 5, the LAD:LCx flow ratio was reduced from 0.89 ± 0.03 at baseline to 0.48 ± 0.04 with placement of the stenosis and during <sup>201</sup>Tl injection (p < 0.001). Furthermore, this ratio remained constant at the time of injection of <sup>99m</sup>Tc-tetrofosmin (0.49 ± 0.05, p = ns versus flow ratio at <sup>201</sup>Tl injection). Hence, microsphere flow did not differ during <sup>201</sup>Tl versus during <sup>99m</sup>Tc-tetrofosmin injection (p = ns).

#### In Vitro Thallium-201 and Technetium-99m-Tetrofosmin Activity

The final LAD:LCx 2-hr <sup>201</sup>Tl activity ratio of 0.66 ± 0.04 was significantly greater than the flow ratio at the time of its injection (0.48 ± 0.04, p < 0.001), indicative of <sup>201</sup>Tl redistribution. The LAD:LCx <sup>99m</sup>Tc-tetrofosmin activity ratio (0.55 ± 0.05) was significantly less (p < 0.05) than the <sup>201</sup>Tl activity ratio (0.66 ± 0.04).

#### Image Defect Ratios

Figure 6 shows examples of background-subtracted left lateral planar images taken at <sup>201</sup>Tl injection, after 2 hr of <sup>201</sup>Tl

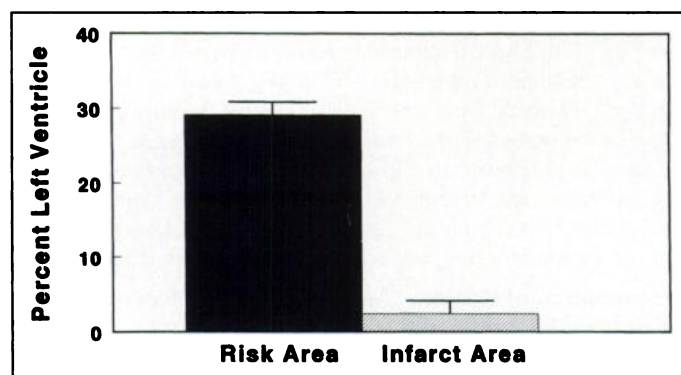


**FIGURE 4.** Mean risk area and infarct size as a percent of the left ventricle as measured by monastral blue dye and triphenyl tetrazolium chloride stain, respectively, confirming a substantial amount of viable myocardium. In six of the nine dogs, infarct size was <1% of the left ventricle.

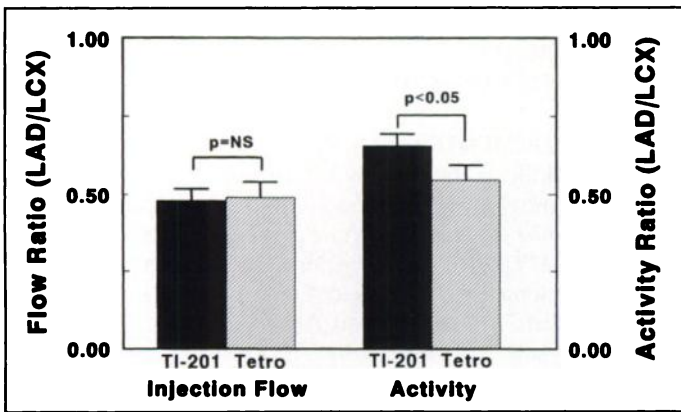


**FIGURE 5.** Comparison of LAD/LCx activity ratios (right panel) for  $^{201}\text{Tl}$  and  $^{99\text{m}}\text{Tc}$ -tetrofosmin in 9 dogs with sustained low flow distal to a severe LAD stenosis. Regional blood flow in the LAD perfusion zone at the time of  $^{201}\text{Tl}$  and  $^{99\text{m}}\text{Tc}$ -tetrofosmin injections was comparable (left panel). Significantly greater  $^{201}\text{Tl}$  than  $^{99\text{m}}\text{Tc}$ -tetrofosmin activity in the asynergic zone of low flow can be observed. LAD = left anterior descending coronary artery; LCX, left circumflex coronary artery; Tetro =  $^{99\text{m}}\text{Tc}$ -tetrofosmin.

redistribution and at  $^{99\text{m}}\text{Tc}$ -tetrofosmin injection. Defect magnitudes are expressed as a ratio of activity in the ischemic LAD region divided by activity in the nonischemic LCx region. In the first example, the  $^{201}\text{Tl}$  defect count ratio was 0.55 initially and 0.66 at 2 hr, indicative of rest redistribution. The initial  $^{99\text{m}}\text{Tc}$ -tetrofosmin defect ratio was 0.54 and, hence, closer to the initial than the delayed  $^{201}\text{Tl}$  defect count ratio. In contrast, in the second example (Fig. 6B), the  $^{99\text{m}}\text{Tc}$ -tetrofosmin defect ratio was more intermediate between the initial and delayed  $^{201}\text{Tl}$  images.

Mean defect count ratios for the nine dogs are depicted in the graph in Figure 7. As shown, the initial and 2-hr delayed mean  $^{201}\text{Tl}$  defect count ratios were  $0.56 \pm 0.02$  and  $0.65 \pm 0.02$ , respectively ( $p < 0.01$ ), indicative of rest redistribution. The

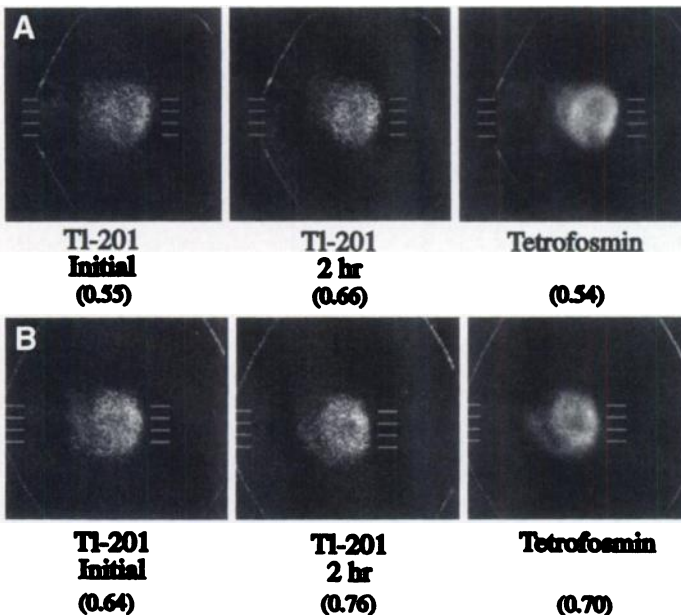


**FIGURE 6.** Background-corrected planar images from two representative dogs. Shown are the initial and 2-hr redistribution  $^{201}\text{Tl}$  images (left, center) and the  $^{99\text{m}}\text{Tc}$ -tetrofosmin image (right). The numbers in parentheses below each image are the defect count ratios derived from image quantification of LAD/LCx count ratios. (A) The  $^{99\text{m}}\text{Tc}$ -tetrofosmin defect count ratio was more similar to the initial, rather than the delayed  $^{201}\text{Tl}$  defect count ratio, whereas in (B) the  $^{99\text{m}}\text{Tc}$ -tetrofosmin defect count ratio was intermediate between the two. LAD = left anterior descending coronary artery; LCx = left circumflex coronary artery.

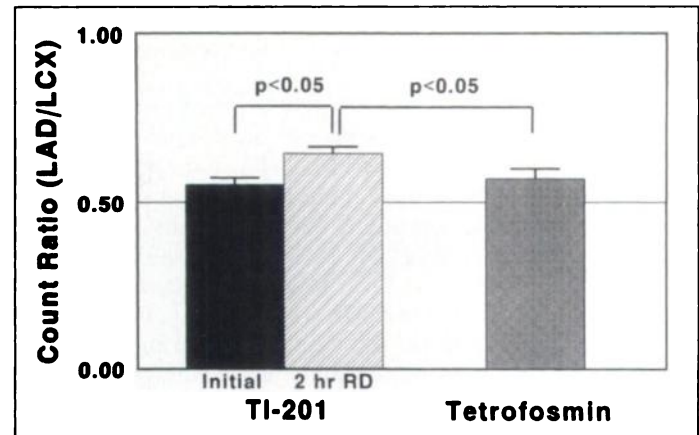


**FIGURE 7.** Initial and 2-hr redistribution (RD)  $^{201}\text{Tl}$  (left bars) versus  $^{99\text{m}}\text{Tc}$ -tetrofosmin (right bar) defect count ratios represented by LAD/LCx count ratios from background-corrected images. Note that substantial  $^{99\text{m}}\text{Tc}$ -tetrofosmin uptake (>50%) occurred in the zone of low flow. LAD = left anterior descending coronary artery; LCX = left circumflex coronary artery.

mean  $^{99\text{m}}\text{Tc}$ -tetrofosmin defect ratio of  $0.57 \pm 0.03$  was comparable to the initial  $^{201}\text{Tl}$  ( $0.56 \pm 0.02$ ,  $p = \text{ns}$ ), but significantly less than the 2-hr  $^{201}\text{Tl}$  defect ratio ( $0.65 \pm 0.02$ ,  $p < 0.05$ ). Like the gamma-well data, although the  $^{99\text{m}}\text{Tc}$ -tetrofosmin defect count ratio was less than the final  $^{201}\text{Tl}$  defect count ratio ( $0.57 \pm 0.03$  versus  $0.65 \pm 0.02$ ,  $p = 0.02$ ), there was substantial uptake of  $^{99\text{m}}\text{Tc}$ -tetrofosmin in the area supplied by the stenotic LAD.

## DISCUSSION

The results of these experiments show that greater resting  $^{201}\text{Tl}$  than  $^{99\text{m}}\text{Tc}$ -tetrofosmin uptake occurs in severely asynergic myocardium in which LAD flow was reduced to approximately 0.5 ml/min/g in an open-chested canine model of sustained anterior wall hypoperfusion. Substantial resting  $^{201}\text{Tl}$  redistribution occurred in this model as assessed by serial quantitative planar imaging. Technetium-99m-tetrofosmin uptake was quantitatively comparable to initial  $^{201}\text{Tl}$  uptake but was significantly less than the 2-hr delayed  $^{201}\text{Tl}$  uptake. Nevertheless, substantial  $^{99\text{m}}\text{Tc}$ -tetrofosmin uptake was detected (average: 57% of normal) in myocardium perfused by the severely stenotic LAD.

These findings are similar to our previous experimental observations using  $^{99\text{m}}\text{Tc}$ -sestamibi in the identical low-flow ischemia model (11). Slightly more  $^{201}\text{Tl}$  rest redistribution was seen in the present experiments than in our previous study comparing  $^{201}\text{Tl}$  uptake with  $^{99\text{m}}\text{Tc}$ -sestamibi uptake. This may be secondary to a slightly greater flow reduction (LAD:LCx flow ratio) at the time  $^{201}\text{Tl}$  was injected in the present experiments (0.48 versus 0.56). The greater the initial flow diminution at the time of  $^{201}\text{Tl}$  administration, the greater the potential for  $^{201}\text{Tl}$  rest redistribution as long as myocardium in the LAD risk area is viable.

Tetrofosmin (1,2-bis[bis(2-ethoxyethyl)phosphino]ethane) forms a lipophilic, cationic complex with  $^{99\text{m}}\text{Tc}$  following incubation of a freeze-dried formulation at room temperature for only 15 min (16). Sinusas et al. (3) showed that  $^{99\text{m}}\text{Tc}$ -tetrofosmin uptake was related to regional myocardial blood flow ( $r = 0.84$ ) in dogs receiving intravenous injection of the tracer in a canine model of ischemia during pharmacologic vasodilatation. As seen with  $^{201}\text{Tl}$  and  $^{99\text{m}}\text{Tc}$ -sestamibi,  $^{99\text{m}}\text{Tc}$ -tetrofosmin activity underestimated flow values above 2.0 ml/min/g. In these experiments,  $^{99\text{m}}\text{Tc}$ -tetrofosmin was shown to clear rapidly from the blood pool with significantly slower myocardial clearance than  $^{201}\text{Tl}$ , as observed with  $^{99\text{m}}\text{Tc}$ -

sestamibi (17). The slow myocardial clearance is the logical explanation for lack of substantial  $^{99m}\text{Tc}$ -tetrofosmin delayed redistribution (8).

Few data are available concerning the use of resting  $^{99m}\text{Tc}$ -tetrofosmin imaging for assessment of myocardial viability in patients with chronic CAD or LV dysfunction or in patients with a recent acute myocardial infarction. Several studies have indicated comparable sensitivity and specificity values for exercise  $^{99m}\text{Tc}$ -tetrofosmin and  $^{201}\text{Tl}$  for detection of CAD (6,10,18–20). In addition, in a group of patients with wall motion abnormalities due to CAD, Senior et al. (21) compared  $^{99m}\text{Tc}$ -tetrofosmin uptake at rest with the improvement in wall thickening assessed by dobutamine echocardiography, and found an 88% concordance for the determination of myocardial viability. The experimental results of the present study suggest that  $^{99m}\text{Tc}$ -tetrofosmin uptake should correlate well with  $^{201}\text{Tl}$  uptake in asynergic underperfused myocardium and yield comparable information relevant to myocardial viability as has been observed in clinical imaging studies at rest using  $^{99m}\text{Tc}$ -sestamibi (22,23). In a recent clinical study, Galassi et al. compared rest-redistribution  $^{201}\text{Tl}$  with rest  $^{99m}\text{Tc}$ -tetrofosmin SPECT in patients with angiographically documented coronary artery disease and severe left ventricular dysfunction (24). The concordance between  $^{201}\text{Tl}$  and  $^{99m}\text{Tc}$ -tetrofosmin for the assessment of myocardial viability (>50% normal uptake) in these patients was 91%.

#### STUDY LIMITATIONS

The goal of comparing  $^{99m}\text{Tc}$ -tetrofosmin uptake with  $^{201}\text{Tl}$  redistribution using imaging as well as in vitro well counting necessitated injecting tetrofosmin 2 hr after  $^{201}\text{Tl}$  so that initial and 2-hr redistribution  $^{201}\text{Tl}$  images could be acquired without contamination by  $^{99m}\text{Tc}$ . Although the experimental preparation remained stable over this period of time, it is possible that the additional 2 hr of sustained low flow between the times that  $^{201}\text{Tl}$  and  $^{99m}\text{Tc}$ -tetrofosmin were administered may have had a greater effect upon tetrofosmin uptake resulting in the slightly lower LAD/LCX count ratio. Recent experimental evidence suggests that the mechanism of uptake of tetrofosmin into myocardial cells is similar to that of sestamibi and involves diffusion into the mitochondria along a large electronegative mitochondrial membrane potential (25,26). When  $^{99m}\text{Tc}$ -sestamibi and  $^{201}\text{Tl}$  were injected simultaneously in the canine model of low flow used in the present study, uptake of  $^{201}\text{Tl}$  was greater than the uptake of  $^{99m}\text{Tc}$ -sestamibi 2 hr after injection of both tracers (11). Thus, the lower uptake of  $^{99m}\text{Tc}$ -tetrofosmin compared to  $^{201}\text{Tl}$  seen in the present experiments is also more likely due to differences in uptake and clearance kinetics between the two agents and not due to a longer duration of ischemia prior to  $^{99m}\text{Tc}$ -tetrofosmin administration.

#### CONCLUSION

In this experimental study in which a sustained >50% reduction in coronary flow and associated profound myocardial asynergy in open-chested anesthetized dogs was produced, greater resting  $^{201}\text{Tl}$  than  $^{99m}\text{Tc}$ -tetrofosmin uptake was observed in the supply zone of the severely stenotic LAD. Nevertheless, substantial  $^{99m}\text{Tc}$ -tetrofosmin uptake (>50% of nonischemic) was seen reflective of significant preserved viability. The slightly higher  $^{201}\text{Tl}$  activity compared to  $^{99m}\text{Tc}$ -tetrofosmin activity in the underperfused LAD zone observed on serial imaging in this canine model of a sustained low flow might not be as evident with in vivo imaging in patients with

ischemic cardiomyopathy because of greater attenuation with  $^{201}\text{Tl}$  compared to a  $^{99m}\text{Tc}$ -labeled agent. Further clinical studies appear warranted to test this supposition.

#### ACKNOWLEDGMENTS

We thank William H. Smith for his assistance in the quantification of myocardial images acquired in this study. We also appreciate the editorial assistance provided by Jerry Curtis in preparing this manuscript. This study was supported by a research grant from Amersham International Inc. and by a grant-in-aid from the Virginia Affiliate, American Heart Association. B.A.K. was supported by an American Heart Association research grant.

#### REFERENCES

1. Glover DK, Ruiz M, Sansoy V, et al. Myocardial uptake of  $^{99m}\text{Tc}$ -tetrofosmin in canine models of coronary occlusion and reperfusion [Abstract]. *Circulation* 1993;88:1–441.
2. Glover DK, Ruiz M, Allen TR, et al. Assessment of myocardial viability by  $^{99m}\text{Tc}$ -tetrofosmin in a canine model of coronary occlusion and reperfusion [Abstract]. *J Am Coll Cardiol* 1994;23:475A.
3. Sinusas AJ, Shi Q, Saltzberg MT, et al. Technetium-99m-tetrofosmin to assess myocardial blood flow: experimental validation in an intact canine model of ischemia. *J Nucl Med* 1994;35:664–671.
4. Hendel RC, Parker MA, Wackers FJ, et al. Reduced variability of interpretation and improved image quality with a technetium-99m myocardial perfusion agent: comparison of thallium-201 and technetium-99m-labeled tetrofosmin. *J Nucl Cardiol* 1994;1:509–514.
5. Takahashi N, Tamaki N, Tadamura E, et al. Combined assessment of regional perfusion and wall motion in patients with coronary artery disease with technetium-99m-tetrofosmin. *J Nucl Cardiol* 1994;1:29–38.
6. Zaret BL, Rigo P, Wackers FJ, et al. Myocardial perfusion imaging with  $^{99m}\text{Tc}$ -tetrofosmin. *Circulation* 1995;91:313–319.
7. Jain D, Wackers FJ, Matterna J, et al. Biokinetics of technetium-99m-tetrofosmin: myocardial perfusion imaging agent: implications for a one-day imaging protocol. *J Nucl Med* 1993;34:1254–1259.
8. Sridhara BS, Braat S, Rigo P, et al. Comparison of myocardial perfusion imaging with technetium-99m-tetrofosmin versus thallium-201 in coronary artery disease. *Am J Cardiol* 1993;72:1015–1019.
9. Jain D, Wackers FJ, McMahon M, Zaret B. Is there any redistribution with  $^{99m}\text{Tc}$ -tetrofosmin imaging? A quantitative study using serial planar imaging [Abstract]. *Circulation* 1992;86:1–46.
10. Tamaki N, Takahashi N, Kawamoto M, et al. Myocardial tomography using technetium-99m-tetrofosmin to evaluate coronary artery disease. *J Nucl Med* 1994;35:594–600.
11. Sansoy V, Glover DK, Watson DD, et al. Comparison of thallium-201 resting redistribution with technetium-99m-sestamibi uptake and functional response to dobutamine for assessment of myocardial viability. *Circulation* 1995;92:994–1004.
12. Sinusas AJ, Trautman KA, Bergin JD, et al. Quantification of area at risk during coronary occlusion and degree of myocardial salvage after reperfusion with technetium-99m-methoxyisobutyl isonitrile. *Circulation* 1990;82:1424–1437.
13. Heymann MA, Payne BD, Hoffman JJ, Rudolph AM. Blood flow measurements with radionuclide-labeled particles. *Prog Cardiovasc Dis* 1977;20:55–79.
14. Smith WH, Watson DD. Technical aspects of myocardial planar imaging with technetium-99m-sestamibi. *Am J Cardiol* 1990;66:16E–22E.
15. Sinusas AJ, Beller GA, Smith WH, et al. Quantitative planar imaging with technetium-99m-methoxyisobutyl isonitrile: comparison of uptake patterns with thallium-201. *J Nucl Med* 1989;30:1456–1463.
16. Higley B, Smith FW, Smith T, et al. Technetium-99m-1,2-bis[bis(2-ethoxyethyl)phosphino]ethane: human biodistribution, dosimetry and safety of a new myocardial perfusion imaging agent. *J Nucl Med* 1993;34:30–38.
17. Okada RD, Glover DK, Gaffney T, Williams S. Myocardial kinetics of technetium-99m-hexakis-2-methoxy-2-methylpropyl-isonitrile. *Circulation* 1988;77:491–498.
18. Sridhara BS, Sochor H, Rigo P, et al. Myocardial single-photon emission computed tomographic imaging with technetium-99m-tetrofosmin: stress-rest imaging with same-day and separate-day rest imaging. *J Nucl Cardiol* 1994;1:138–143.
19. Nakajima K, Taki J, Shuke N, et al. Myocardial perfusion imaging and dynamic analysis with technetium-99m-tetrofosmin. *J Nucl Med* 1993;34:1478–1484.
20. Rigo P, Leclercq B, Itti R, et al. Technetium-99m-tetrofosmin myocardial imaging: a comparison with thallium-201 and angiography. *J Nucl Med* 1994;35:587–593.
21. Senior R, Kaul S, Raval U, et al. Is  $^{99m}\text{Tc}$ -tetrofosmin myocardial uptake an indicator of myocardial viability [Abstract]. *Br Heart J* 1995;3:P28.
22. Udelson JE, Coleman PS, Metherall J, et al. Predicting recovery of severe regional ventricular dysfunction. Comparison of resting scintigraphy with  $^{201}\text{Tl}$  and  $^{99m}\text{Tc}$ -sestamibi. *Circulation* 1994;89:2552–2561.
23. Kauffman GJ, Boyne TS, Watson DD, et al. Quantitative comparison of rest Tl-201 SPECT and rest Tc-99m-sestamibi SPECT imaging in patients with severe left ventricular dysfunction [Abstract]. *Circulation* 1994;90:1–315.
24. Galassi AR, Centamore G, Liberti F, et al. Quantitative SPECT Tc-99m-tetrofosmin for the assessment of myocardial viability in patients with severe left ventricular dysfunction [Abstract]. *J Nucl Cardiol* 1995;2:S23.
25. Songadele JA, Younes A, Maublant JC, et al. Role of active mechanisms in the mitochondrial retention of  $^{99m}\text{Tc}$ -tetrofosmin. [Abstract]. *Circulation* 1994;90:1–76.